AIMS Mathematics, 8(1): 2435−2452.
DOI: 10.3934/math.2023126
Received: 07 July 2022
Revised: 17 September 2022
Accepted: 28 September 2022
Published: 03 November 2022

http://www.aimspress.com/journal/Math

Research article

Artificial neural network procedures for the waterborne spread and control of diseases

Naret Ruttanaprommarin[1], Zulqurnain Sabir[2,3], Rafaél Artidoro Sandoval Núñez[4], Soheil Salahshour[5], Juan Luis García Guirao[6], Wajaree Weera[7], Thongchai Botmart[7,*] and Anucha Klamnoi[8]

[1] Department of Science and Mathematics, Faculty of Industry and Technology, Rajamangala University of Technology Isan Sakonnakhon Campus, Sakonnakhon 47160, Thailand
[2] Department of Mathematics and Statistics, Hazara University, Mansehra, Pakistan
[3] Department of Mathematical Sciences, United Arab Emirates University, P.O. Box 15551, Al Ain, UAE
[4] Universidad Nacional Autónoma de Chota, Cajamarca, Perú
[5] Faculty of Engineering and Natural Sciences, Bahcesehir University, Istanbul, Turkey
[6] Technical University of Cartagena, Applied Mathematics and Statistics Department, Spain
[7] Department of Mathematics, Faculty of Science, Khon Kaen University, Khon Kaen 40002, Thailand
[8] Department of Applied Mathematics and Statistics, Rajamangala University of Technology Isan, Nakhon Ratchasima 30000, Thailand

* **Correspondence:** Email: thongbo@kku.ac.th.

Abstract: In this study, a nonlinear mathematical SIR system is explored numerically based on the dynamics of the waterborne disease, e.g., cholera, that is used to incorporate the delay factor through the antiseptics for disease control. The nonlinear mathematical SIR system is divided into five dynamics, susceptible $X(u)$, infective $Y(u)$, recovered $Z(u)$ along with the $B(u)$ and $C_h(u)$ be the contaminated water density. Three cases of the SIR system are observed using the artificial neural network (ANN) along with the computational Levenberg-Marquardt backpropagation (LMB) called ANNLMB. The statistical performances of the SIR model are provided by the selection of the data as 74% for authentication and 13% for both training and testing, together with 12 numbers of neurons. The exactness of the designed ANNLMB procedure is pragmatic through the comparison procedures of the proposed and reference results based on the Adam method. The substantiation, constancy,

reliability, precision, and ability of the proposed ANNLMB technique are observed based on the state transitions measures, error histograms, regression, correlation performances, and mean square error values.

Keywords: SIR system; delay term; artificial neural network; stochastic procedure; Levenberg-Marquardt backpropagation
Mathematics Subject Classification: 34K50, 92B20

1. Introduction

The number of deaths worldwide is around 4500 among children at a young age based on waterborne diseases like typhoid, hepatitis E, cholera, hepatitis A, Shigella, and giardiasis [1−6]. The pathogens based on such diseases provide the aquatic environment using the wastes or feces of symptomatic or asymptomatic diseased animals or persons and pollute it-consuming dirty water for waterborne illnesses like cholera. From the start, cholera was considered an epidemic based on fecaloral transmission. However, Snow's influential investigations [7], proved that ingesting contaminated water by the susceptible is a significant reason for the spreading of cholera contagion [8]. In the mid of the 18^{th} century, Filippo Pacini proved the occurrence of Vibrio cholerae (V) in polluted water [9]. After 30 years, these investigations were performed by Robert Koch with V cholerae in humans [10]. They accrue an enterotoxin yield that represents diarrhea, acidosis, and vomiting. A person faces terrible health due to the lack of proper treatment, and death may occur. The V cholerae permanence for the water environment was considered in the last quarter of the 19^{th} century. A few years later, it was proved that the V cholerae could be survived for a long time in freshwater [11]. A reservoir comprises dirty water, where V cholerae is accountable for the epidemic based on cholera. Most developing countries faces cholera disease based on inadequate hygiene, inadequate supply of safe water and inappropriate treatment of reservoirs. In the sixth decade of the last century, the 7^{th} phase of the pandemic, cholera started in the Indonesian region and spread worldwide. Most Asian and African countries are still facing this disease. Fifteen years ago, the clear cholera cases were 177,963 with 4031 deaths in 53 countries, where 99% of cases were reported in the African regions [12]. In recent years, cholera again spread in Haiti after one century spreading rapidly with 452,189 positive cases and 6334 deaths [13].

Many SIS and SIRS systems, have been discovered and examined in the last few years to recognize the spread dynamics based on transferrable diseases [14−20]. Based on these systems, it is accessed that the disease spreads directly between the susceptible and the infectives. Cholera disease is not a spreading virus from one person to another. Consequently, direct interaction with healthy individuals is not a danger of contracting the infection, whereas healthy individuals can contract the infection by drinking dirty water in the presence of the V cholerae. There have been many investigations that present the cholera disease dynamics [21−25]. Capasso et al. designed the mathematical formulation to provide the dynamics of cholera occurrences in Italy. Codeco presented this system to investigate the water reservoir based on cholera. Pascual et al. proposed Codec-o's system by incorporating of another model to describe the water volume with V cholera. Hartley et al. provided the Codec-o's system to consider the hyper infectious bacterium's role in the cholera spread. Jensen et al. investigated the bacteriophage, role in controlling cholera outbreaks. Earn et al. formulated a

mathematical model to investigate waterborne disease dynamics, like Campylobacter, giardiasis, hepatitis A and hepatitis E. The current modeling shows the infection between susceptible and infectives and the dirty water supply, including pathogens. Recently, Tian and Wang proposed a nonlinear cholera system to consider the standard incidence function based on the multiple spreads along with the function's growth rate using the pathogens.

The experience provides that the occurrence of diseases based on waterborne infection produces mortality in millions and a massive amount of money in disease control and health care. Healthcare organizations have formulated numerous strategies to prevent epidemics, like awareness, vaccination, and quarantine. Various vaccination systems have been presented to prevent and control epidemics [26−30]. In recent years, Misra provided a mathematical system to provide the awareness driven by the media based on the occurrence of infectious viruses. The outbreaks of cholera in Haiti have been examined in the references [31,32]. These investigations provide a more promising structure based on the potential effects of different control stratagems for cholera, like vaccination, the establishment of clean and safe drinking water, proper sanitation, minimizing scarcity based on the decontaminated food, good sewage model to excreta clearance and wastage of water conduct.

The motive of this research study is to provide a nonlinear mathematical SIR system based on the dynamics of waterborne disease. The mathematical SIR nonlinear system is categorized into five dynamics, susceptible $X(u)$, infective $Y(u)$, recovered $Z(u)$, along with the $B(u)$ and $C_h(u)$, be the contaminated water density containing the pathogen. The solutions of the SIR system are provided by using the stochastic artificial neural network (ANN) along with the computational Levenberg-Marquardt backpropagation (LMB) called ANNLMB. The stochastic computing performances have been used to solve several complicated models, such as food supply systems [33,34], the coronavirus dynamical models [35], dynamical HIV systems [36], thermal explosion theory [37], eye surgery systems [38,39], singular differential systems [40] and smoking differential systems [41]. The novel features of the proposed investigations are signified as:

- A mathematical SIR system is explored numerically using the dynamics of the waterborne disease, e.g., cholera, and is analyzed to incorporate the delay factor by using the antiseptics for disease control.
- The mathematical SIR model, numerical performances are presented using the stochastic procedures based on the ANNLMB.
- Three different cases based on the mathematical SIR delay model are numerical stimulated through the proposed stochastic structure of the ANNLMB.
- The correctness of the computing ANNLMB solver is authenticated by comparing the obtained and reference results.
- The trustworthiness of the ANNLMB numerical method is obtained by using the absolute error (AE) performances for solving the mathematical SIR delay differential model.
- The performances of the state transitions (STs) measures, error histograms (EHs), regression, correlation performances, and MSE values are provided through the ANNLMB computing approach scheme for solving the mathematical SIR delay differential model.

The rest of the paper is organized as follows: The mathematical formulations of the SIR delay differential model are provided in Section 2. Then, the proposed stochastic structure is given in Section 3. Next, the results simulations are provided in Section 4. Finally, the concluding remarks are presented in Section 5.

2. Mathematical model

This study section presents the mathematical formulations of the nonlinear SIR delay differential model. First, the mathematical form of the SIR system is given in system (1), while the parameter details are provided in Table 1 [42].

$$\begin{cases} \dfrac{dX(u)}{du} = \alpha - \beta X(u)B(u) - \delta X(u) + dZ(u) & X(0) = i_1, \\ \dfrac{dY(u)}{du} = \beta X(u)B(u) - (\delta + A + \upsilon)Y(u) & Y(0) = i_2, \\ \dfrac{dZ(u)}{du} = \upsilon Y(u) - (\delta + d)Z(u) & Z(0) = i_3, \\ \dfrac{dB(u)}{du} = \mu Y(u) - \mu_1 B(u) - \phi N(u)B(u) - \sigma_2 B(u)C_h(u) & B(0) = i_4, \\ \dfrac{dC_h(u)}{du} = \theta B(u-\tau) - \theta_1 C_h(u) - \sigma_1 B(u)C_h(u) & C_h(0) = i_5. \end{cases} \tag{1}$$

Table 1. Description of the parameters based on the SIR mathematical delay differential model.

Parameters	Details
$X(u)$	Susceptible
$Y(u)$	Infected
$Z(u)$	Recovered
β	The transmission rate of susceptibility to an infective category based on the contaminated water consumption
A	Disease death ratio
α	Constant birth and immigration rates based on the susceptible population
δ	Natural death rate
θ	Introduction rate of disinfectants
υ	Infective rate to be recovered
μ	Growth rate based on the density of V
μ_1	The natural decay rate of V
σ_1	Absorption disinfectants rate
θ_1	Natural disaster rate
σ_2	The decay rate of V
τ	Delay term
ϕ	Cholerae
u	Time
i_1, i_2, i_3, i_4, i_5	Initial conditions

3. Stochastic computing ANNLMB procedure

This section presents the ANNLMB computing procedure for solving the SIR mathematical delay differential model is given as:

- The actual operator performances through the ANNLMB computing solver are presented.
- The execution procedures using the ANNLMB stochastic scheme are derived to solve the SIR mathematical delay differential model.

Table 2 states the parameters for the SIR mathematical delay differential model based on the ANNLMB stochastic scheme. Minor modification and adjustment can lead to subpar results or premature convergence. As a result, these alternatives will be appropriately included following extensive numerical testing and knowledge. The data is used between 0 and 1 with the 0.01 step size, and the Matlab built-in command nftool is applied to solve the SIR mathematical delay differential model.

Table 2. The setting of the parameters to implement the ANNLMB scheme.

Index	Settings
Hidden neurons	12
Fitness (MSE)	0
Statics selection	Random
Maximum Epochs	1000
Decreasing values of Mu	0.2
Test data	13%
Mu maximum performances	10^{08}
Train data	13%
Generation of dataset	Adam approach
Adaptive parameter	0.002
Hidden/output/input layers construction	Single
Increasing mu performances	9
Verification data	74%
Authentication count fails	7
Minimum values of the gradient	10^{-07}
Execution of Adam and dismissing standards	Default

The numerical computing values using three different deviations of the SIR mathematical delay differential model based on the ANNLMB stochastic scheme. The SIR mathematical delay differential model is presented with the data selection as 74% for authentication and 13% for training and testing together with 12 neurons. The construction of the input, hidden layer, output layer, and output is provided in Figure 1. Figure 2 signifies the optimization procedures based on the multi-layer performances of the stochastic ANNLMB solver.

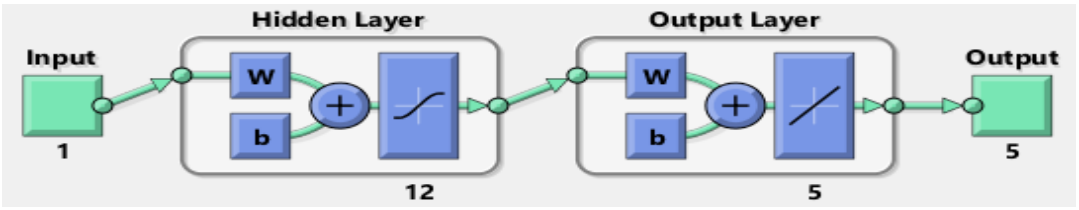

Figure 1. Input, hidden layer, output, and output of the mathematical delay differential system are derived through the proposed ANNLMB scheme.

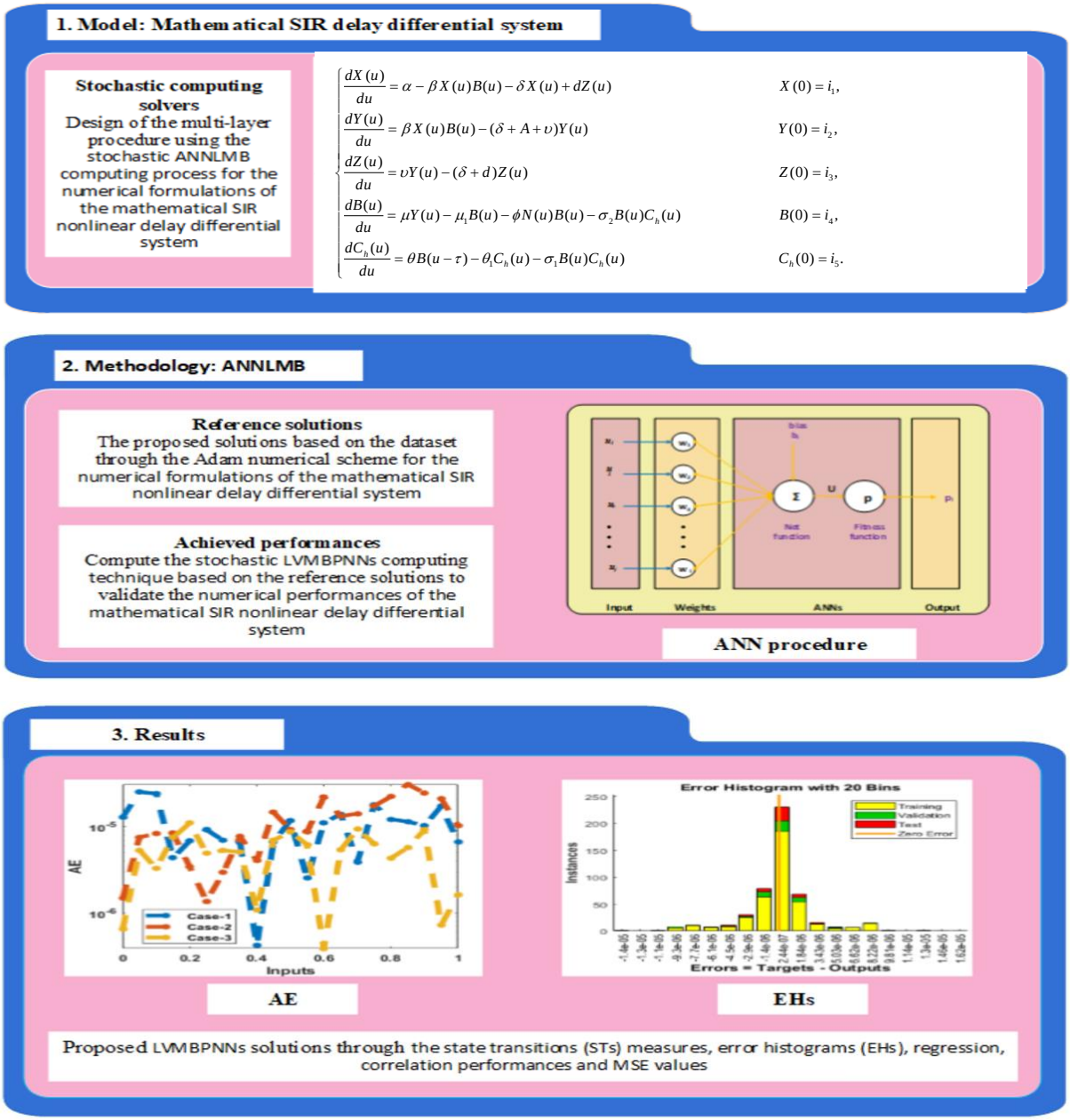

Figure 2. Designed ANNLMB computing solver for solving the SIR mathematical delay differential system.

4. Discussion

This section presents the numerical representations of the SIR mathematical delay differential system using the stochastic computing ANNLMB solver. The mathematical depictions of each case are presented as:

Case 1: Suppose $\alpha = 10$, $\beta = 0.0000001$, $\upsilon = 0.2$, $\delta = 0.00005$, $d = 0.001$, $\mu = 25$, $\mu_1 = 0.03$, $\phi = 0.000002$ $\sigma_2 = 0.99$, $\sigma = 0.001$, $\theta_1 = 1$, $\sigma_1 = 0.0004$, $N(u) = 0.1$, $\tau = 0.1$, $i_1 = 0.1$, $i_2 = 0.2$, $i_3 = 0.3$, $i_4 = 0.4$, and $i_5 = 0.5$ is used in the system (1) as follows:

$$\begin{cases} \frac{dX(u)}{du} = 10 - \left(1\times10^{-07}\right)X(u)B(u) - \left(5\times10^{-05}\right)X(u) + \left(1\times10^{-03}\right)Z(u) & X(0) = 0.1, \\ \frac{dY(u)}{du} = (\left(1\times10^{-07}\right)X(u)B(u) - 10.20005Y(u) & Y(0) = 0.2, \\ \frac{dZ(u)}{du} = 0.2Y(u) - 0.001001Z(u) & Z(0) = 0.3, \\ \frac{dB(u)}{du} = 25Y(u) - \left(3\times10^{-02}\right)B(u) - \left(2\times10^{-08}\right)B(u) - (0.99)B(u)C_h(u) & B(0) = 0.4, \\ \frac{dC_h(u)}{du} = \left(2\times10^{-06}\right)B(u-0.1) - C_h(u) - \left(4\times10^{-04}\right)B(u)C_h(u) & C_h(0) = 0.5. \end{cases} \tag{2}$$

Case 2: Suppose $\alpha = 10$, $\beta = 0.0000001$, $\upsilon = 0.2$, $\delta = 0.00005$, $d = 0.001$, $\mu = 25$, $\mu_1 = 0.03$, $\phi = 0.000002$, $\sigma_2 = 0.99$, $\sigma = 0.001$, $\theta_1 = 1$ $\sigma_1 = 0.0004$, $N(u) = 0.1$, $\tau = 0.1$, $i_1 = 0.2$, $i_2 = 0.3$, $i_3 = 0.4$, $i_4 = 0.5$, and $i_5 = 0.6$ is used in the system (1) as follows:

$$\begin{cases} \frac{dX(u)}{du} = 10 - \left(1\times10^{-07}\right)X(u)B(u) - \left(5\times10^{-05}\right)X(u) + \left(1\times10^{-03}\right)Z(u) & X(0) = 0.2, \\ \frac{dY(u)}{du} = (\left(1\times10^{-07}\right)X(u)B(u) - 10.20005Y(u) & Y(0) = 0.3, \\ \frac{dZ(u)}{du} = 0.2Y(u) - 0.001001Z(u) & Z(0) = 0.4, \\ \frac{dB(u)}{du} = 25Y(u) - \left(3\times10^{-02}\right)B(u) - \left(2\times10^{-08}\right)B(u) - (0.99)B(u)C_h(u) & B(0) = 0.5, \\ \frac{dC_h(u)}{du} = \left(2\times10^{-06}\right)B(u-0.1) - C_h(u) - \left(4\times10^{-04}\right)B(u)C_h(u) & C_h(0) = 0.6. \end{cases} \tag{3}$$

Case 3: Suppose $\alpha = 10$, $\beta = 0.0000001$, $\upsilon = 0.2$, $\delta = 0.00005$, $d = 0.001$, $\mu = 25$, $\mu_1 = 0.03$, $\phi = 0.000002$, $\sigma_2 = 0.99$, $\sigma = 0.001$, $\theta_1 = 1$ $\sigma_1 = 0.0004$, $N(u) = 0.1$, $\tau = 0.1$, $i_1 = 0.3$, $i_2 = 0.4$, $i_3 = 0.5$, $i_4 = 0.6$, and $i_5 = 0.7$ is used in the system (1) as follows:

$$\begin{cases} \frac{dX(u)}{du} = 10 - \left(1\times10^{-07}\right)X(u)B(u) - \left(5\times10^{-05}\right)X(u) + \left(1\times10^{-03}\right)Z(u) & X(0) = 0.3, \\ \frac{dY(u)}{du} = \left(\left(1\times10^{-07}\right)X(u)B(u) - 10.20005Y(u)\right. & Y(0) = 0.4, \\ \frac{dZ(u)}{du} = 0.2Y(u) - 0.001001Z(u) & Z(0) = 0.5, \\ \frac{dB(u)}{du} = 25Y(u) - \left(3\times10^{-02}\right)B(u) - \left(2\times10^{-08}\right)B(u) - (0.99)B(u)C_h(u) & B(0) = 0.6, \\ \frac{dC_h(u)}{du} = \left(2\times10^{-06}\right)B(u-0.1) - C_h(u) - \left(4\times10^{-04}\right)B(u)C_h(u) & C_h(0) = 0.7. \end{cases} \tag{4}$$

The values based on the numerical procedures of the mathematical delay differential system are derived through the proposed ANNLMB scheme and are plotted in Figures 3−5. The best validation performances based on the MSE are provided in Figure 3a−c, while the gradient, Mu, and validation checks based on STs values are provided in Figure 3d−f. The best validation measures using the mathematical SIR delay differential model are illustrated at epochs 958 for Case 1, whereas 1000 iterations for Cases 2 and 3. The performances have been calculated around 5.7035×10^{-11}, 1.312×10^{-10} and 1.8378×10^{-11}, respectively. The gradient operators have been derived as 9.9661×10^{-08}, 1.3471×10^{-07} and 1.9157×10^{-07} for the mathematical SIR delay differential model. These graphical illustrations present the convergence of the statistical ANNLMB process to solve the SIR mathematical form of the delay differential model. Figure 4a−c performs the results assessments based on training targets, training outputs, validation targets, validation outputs, test targets, test outputs, errors, and fitness performances. These graphical measures indicate the result comparisons for each case of the SIR mathematical form of the delay differential model. The EHs based on the training, validation, test and zero error for each case of the SIR mathematical form of the delay differential model are provided in Figure 4d−f using the stochastic ANNLMB measures. The EHs performances have been derived as 4.87×10^{-08}, 2.64×10^{-06} and 2.44×10^{-07} for each case of the SIR mathematical form of the delay differential model. The regression plots are derived in Figure 5 based on the training, validation, and testing performances for the mathematical SIR delay differential model. The correlation plots 1 for each case of the mathematical SIR delay differential model using the stochastic ANNLMB technique. Based on the validation, training, and testing these measures authenticate the exactness of the stochastic ANNLMB scheme to solve the mathematical SIR delay, differential model. The MSE convergence via validation, generations, training, testing, complexity, and backpropagation is presented in Table 3 based on the ANNLMB solver.

Table 3. Design statics via ANNLMB solver for the mathematical delay differential system.

Case	MSE			Gradient	Mu	Iterations	Performance	Time
	Testing	Training	Endorsement					
(1)	1.13×10^{-10}	5.90×10^{-11}	5.70×10^{-11}	1.00×10^{-07}	1×10^{-08}	958	5.91×10^{-11}	02 Sec
(2)	3.11×10^{-10}	1.08×10^{-10}	1.31×10^{-10}	1.35×10^{-07}	$1\times10^{--08}$	1000	1.08×10^{-10}	03 Sec
(3)	1.13×10^{-11}	1.11×10^{-11}	1.83×10^{-11}	1.92×10^{-07}	1×10^{-09}	1000	1.11×10^{-11}	03 Sec

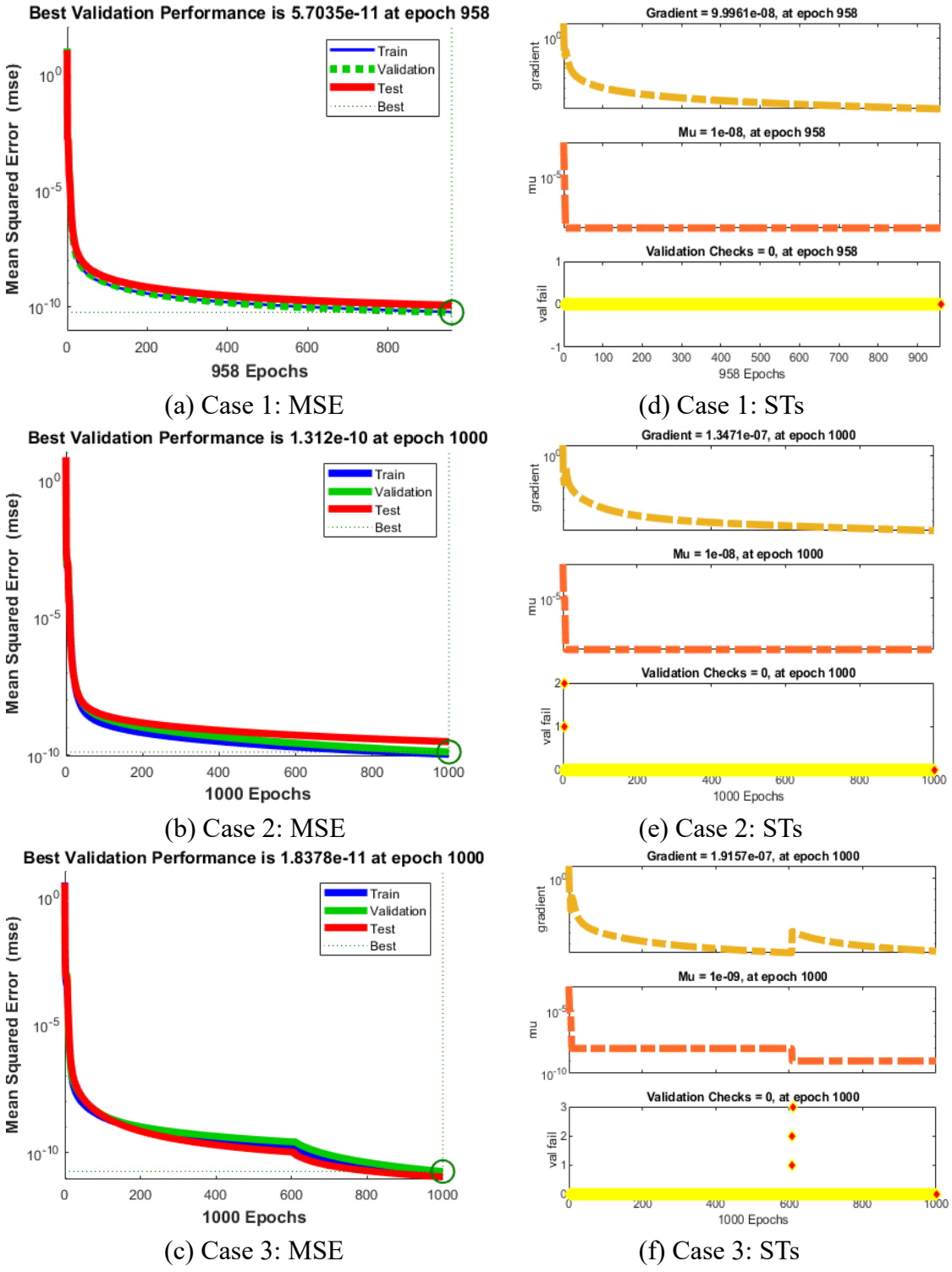

(a) Case 1: MSE (d) Case 1: STs

(b) Case 2: MSE (e) Case 2: STs

(c) Case 3: MSE (f) Case 3: STs

Figure 3. MSE and STs values through the ANNLMB stochastic procedure for the mathematical SIR delay differential model.

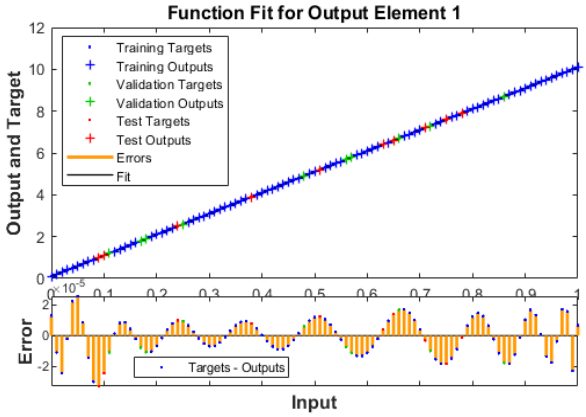

(a) Case 1: Results

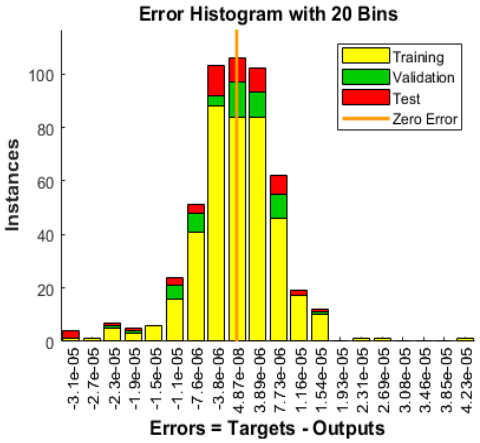

(d) Case 1: EHs

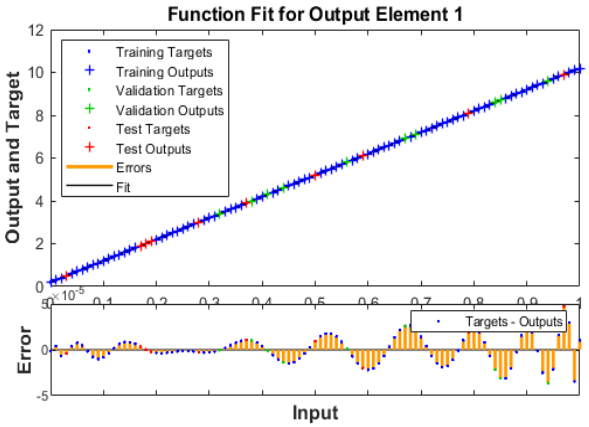

(b) Case 2: Results

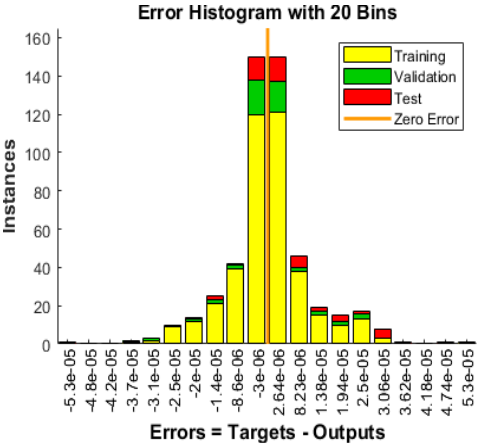

(e) Case 2: EHs

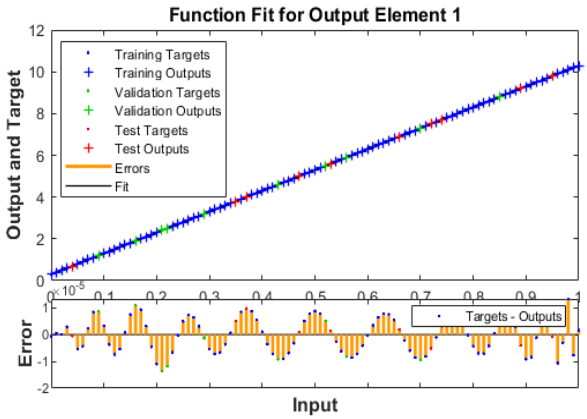

(c) Case 3: Results

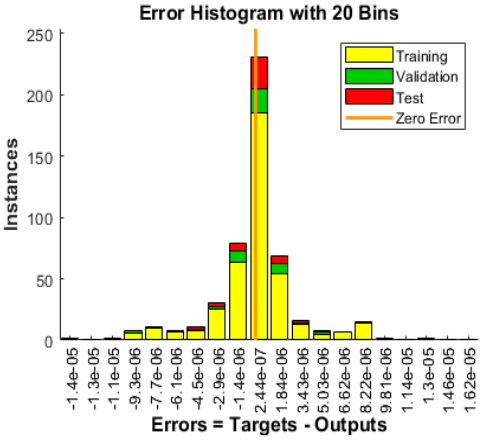

(f) Case 3: EHs

Figure 4. Result assessments and EHs measures for the mathematical SIR delay differential model.

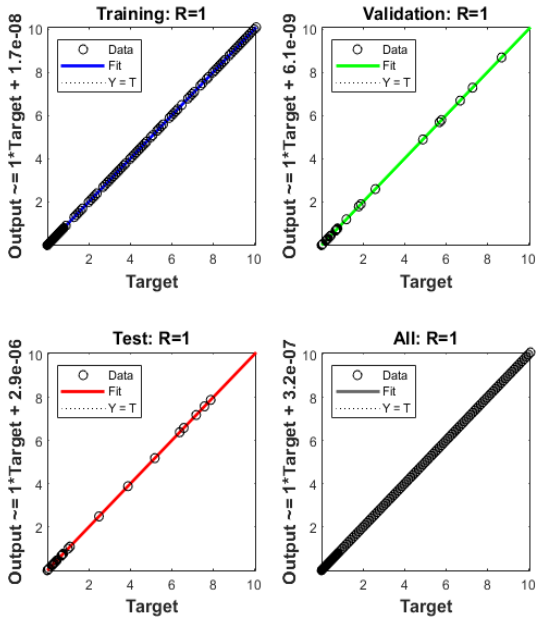

(a) Regression: Case 1

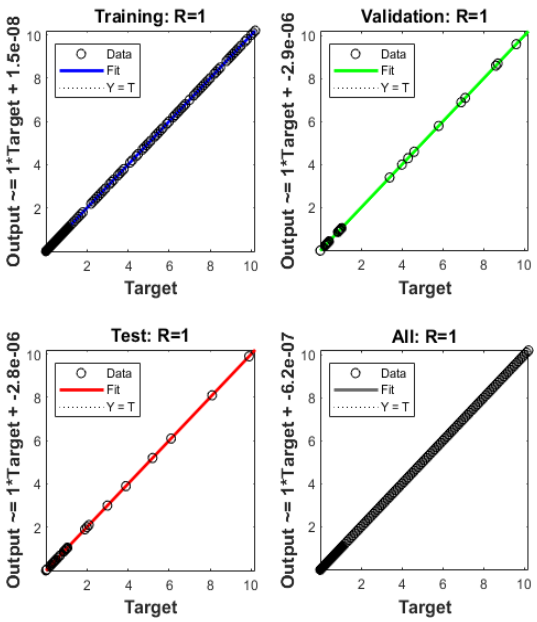

(b) Regression: Case 2

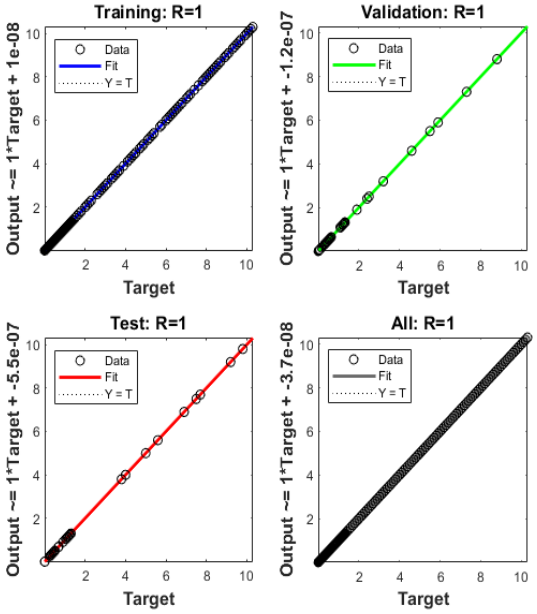

(c) Regression: Case 3

Figure 5. Regression values for the mathematical SIR delay differential model.

The comparison of the results and the absolute error (AE) for three different cases of the mathematical SIR delay differential model using the ANNLMB stochastic procedure is provided in Figures 6 and 7. These plots authenticate the exactness of the stochastic ANNLMB method for solving the mathematical SIR delay differential model. Figure 6 compares the obtained and reference results for the mathematical SIR delay differential model based on the stochastic ANNLMB scheme. The obtained and reference overlapping of the results indicates the correctness of the ANNLMB method to solve the obtained and reference solutions. The AE values based on three different deviations of the mathematical SIR delay differential model are provided in Figure 7. The mathematical SIR system is divided into five dynamics, susceptible $X(u)$, infective $Y(u)$, recovered $Z(u)$ along with the $B(u)$ and $C_h(u)$ be the contaminated water density containing pathogen V. The AE for susceptible $X(u)$ is

calculated as 10^{-05} to 10^{-06}, 10^{-06} to 10^{-05}, and 10^{-06} to 10^{-05} for individual cases of the mathematical SIR delay differential model. The AE of the infective $Y(u)$ is found as 10^{-05} to 10^{-06}, 10^{-05} to 10^{-06} and 10^{-05} to 10^{-08} for individual cases of the mathematical SIR delay differential model. The AE for the recovered $Z(u)$ are found as 10^{-04} to 10^{-06}, 10^{-04} to 10^{-05}, and 10^{-06} to 10^{-07} for individual cases of the mathematical SIR delay differential model. The values based on the $B(u)$ are found as 10^{-05} to 10^{-08}, 10^{-05} to 10^{-07} and 10^{-06} to 10^{-07}, while the $C_h(u)$ values are calculated as 10^{-05} to 10^{-06}, 10^{-05} to 10^{-06}, and 10^{-06} to 10^{-07} mathematical SIR delay differential model. These accurate performances indicate the correctness and exactness of the stochastic ANNLMB method for the mathematical SIR delay differential model.

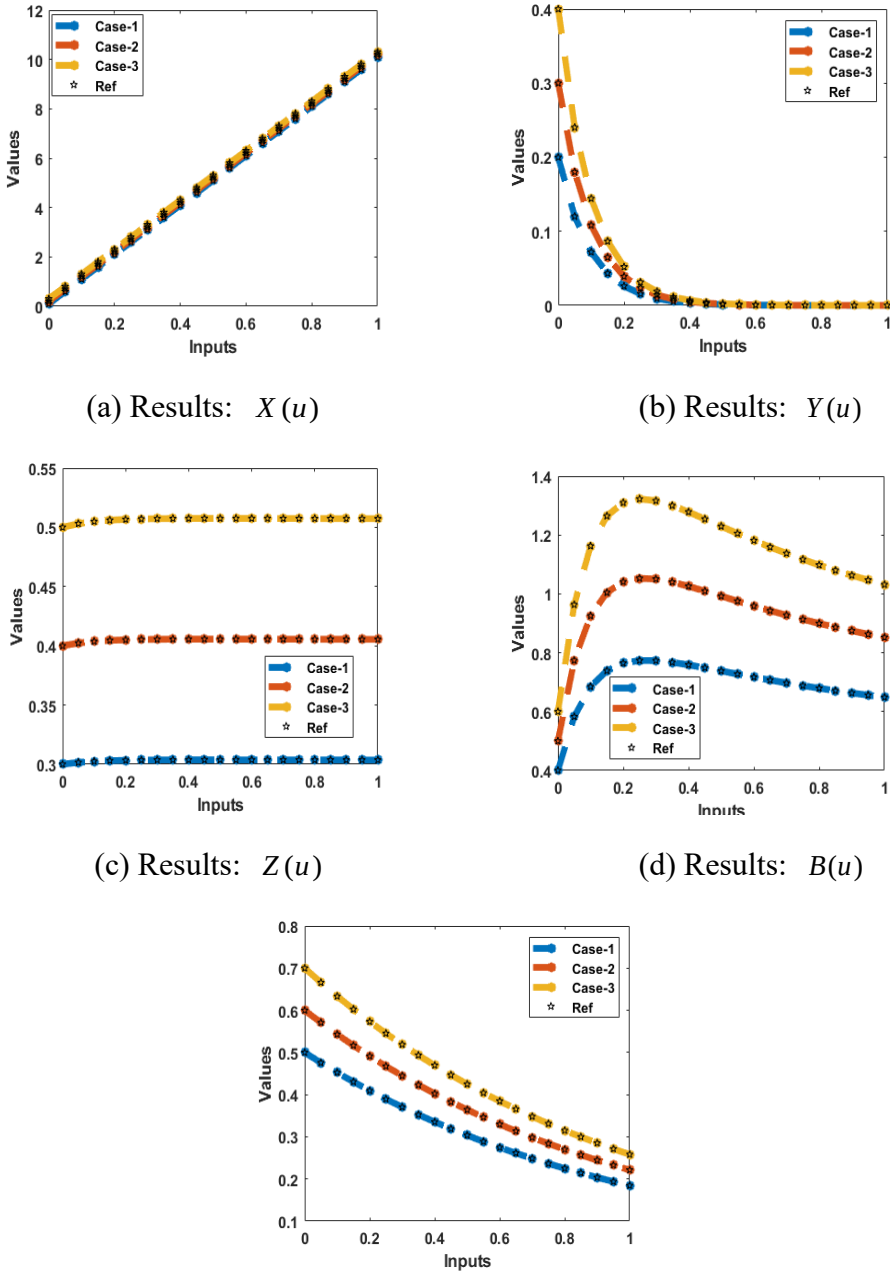

(a) Results: $X(u)$ (b) Results: $Y(u)$

(c) Results: $Z(u)$ (d) Results: $B(u)$

(e) Results: $C_h(u)$

Figure 6. Comparison performances for the mathematical SIR delay differential model.

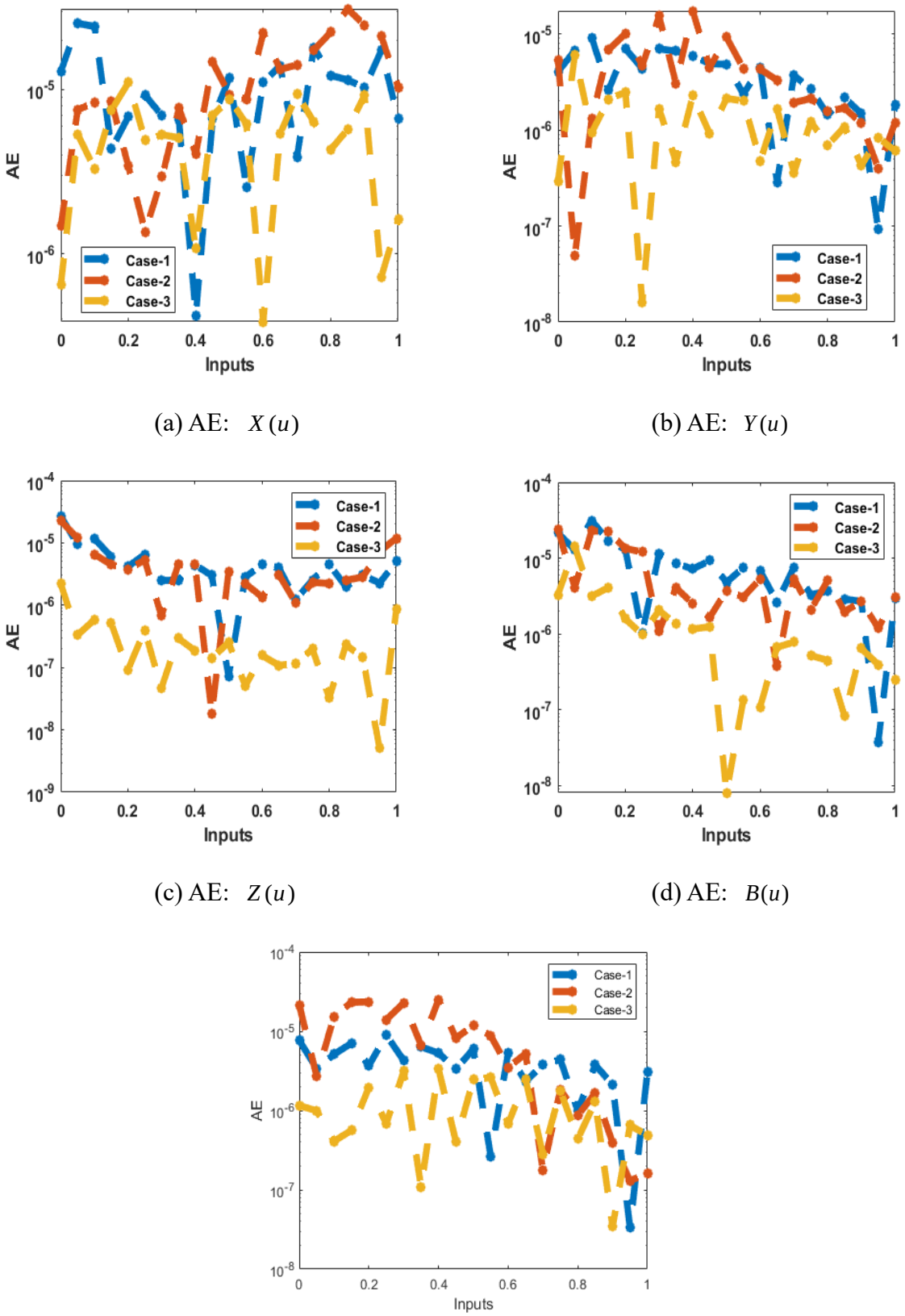

(a) AE: $X(u)$ (b) AE: $Y(u)$

(c) AE: $Z(u)$ (d) AE: $B(u)$

(e) AE: $C_h(u)$

Figure 7. AE performances for the mathematical SIR delay differential model.

5. Conclusions

These investigations aim to perform the numerical performances of the SIR mathematical delay differential system using the proposed ANNLMB method. The nonlinear mathematical SIR system is divided into five dynamics, susceptible $X(u)$, infective $Y(u)$, recovered $Z(u)$, along with the $B(u)$ and $C_h(u)$, be the contaminated water density containing the pathogen. Finally, some concluding remarks on current work are presented:

- The mathematical form of the SIR system has been presented by using the dynamics of the waterborne disease to incorporate the delay factor with the antiseptics for disease control.
- The numerical performances for three cases of the mathematical SIR delay differential model have been presented using the stochastic procedures based on the ANNLMB.
- The data selection provides statistic procedures for solving the SIR mathematical delay differential model as 74% for authentication and 13% for both training and testing together with 12 numbers of neurons.
- The correctness of the computing ANNLMB solver has been authenticated by comparing of the obtained and reference results.
- The reliability of the ANNLMB numerical scheme is obtained through the absolute error performances, which are found as 10^{-06} to 10^{-07} for individual cases of the mathematical SIR delay differential model.
- The performances of the state transition, error histograms, regression, correlation, and MSE values are provided through the ANNLMB computing scheme for solving the mathematical SIR delay differential model.
- The delay term in the mathematical SIR differential model is challenging to handle. Therefore the ANNLMB stochastic scheme is an excellent choice to present the numerical simulations.

In upcoming studies, the ANNLMB stochastic scheme can be implemented to solve the fractional models [43−47], biological systems [48,49] and fluid dynamical models [50−53], and many more [54−56].

Acknowledgments

This research received funding support from the NSRF via the Program Management Unit for Human Resources & Institutional Development, Research and Innovation [grant number B05F650018].

Conflict of interest

All authors declare that there are no potential conflicts of interest.

References

1. T. Butler, J. Knight, S. K. Nath, P. Speelman, S. K. Roy, M. A. K. Azad, Typhoid fever complicated by intestinal perforation: A persisting fatal disease requiring surgical management, *Rev. Infect. Dis.*, **7** (1985), 244−256. https://doi.org/10.1093/clinids/7.2.244

2. A. B. Labrique, S. S. Sikder, L. J. Krain, K. P. West Jr, P. Christian, M. Rashid, et al., A vaccine-preventable cause of maternal deaths, *Emerg. Infect. Dis.*, **18** (2012), 1401−1404. https://doi.org/10.3201/eid1809.120241
3. A. K. Siddique, K. Akram, K. Zaman, S. Laston, A. Salam, R. N. Majumdar, et al., Why treatment centres failed to prevent cholera deaths among Rwandan refugees in Goma, Zaire, *Lancet*, **345** (1995), 359−361. https://doi.org/10.1016/S0140-6736(95)90344-5
4. D. E. Snider Jr, G. J. Caras, Isoniazid-associated Hepatitis deaths: A review of available information, *Am. Rev. Respir. Dis.*, **145** (1992), 494−497. https://doi.org/10.1164/ajrccm/145.2_Pt_1.494
5. P. Bardhan, A. S. G. Faruque, A. Naheed, D. A. Sack, Decreasing shigellosis-related deaths without Shigella spp.-specific interventions, Asia, *Emerg. Infect. Dis.*, **16** (2010), 1718−1723. https://doi.org/10.3201/eid1611.090934
6. G. Corrêa, R. Vilela, R. F. Menna-Barreto, V. Midlej, M. Benchimol, Cell death induction in Giardia lamblia: Effect of beta-lapachone and starvation, *Parasitol. Int.*, **58** (2009), 424−437. https://doi.org/10.1016/j.parint.2009.08.006
7. J. Snow, B. W. Richardson, Snow on cholera: Being a reprint of two papers, *JAMA*, **108** (1937), 421. https://doi.org/10.1001/jama.1937.02780050077036
8. A. R. Tuite, C. H. Chan, D. N. Fisman, Cholera, canals, and contagion: Rediscovering Dr Beck's report, *J. Public Health Pol.*, **32** (2011), 320−333. https://doi.org/10.1057/jphp.2011.20
9. G. Donatelli, A. Spota, F. Cereatti, S. Granieri, I. Dagher, R. Chiche, et al., Endoscopic internal drainage for the management of leak, fistula, and collection after sleeve gastrectomy: Our experience in 617 consecutive patients, *Surg. Obes. Relat. Dis.*, **17** (2021), 1432−1439. https://doi.org/10.1016/j.soard.2021.03.013
10. D. Lippi, E. Gotuzzo, The greatest steps towards the discovery of Vibrio cholerae, *Clin. Microbiol. Infect.*, **20** (2014), 191−195. https://doi.org/10.1111/1469-0691.12390
11. R. J. Borroto, Ecology of Vibrio cholerae serogroup 01 in aquatic environments, *Rev. Panam. Salud Publ.*, **2** (1997), 328−333. https://doi.org/10.1590/s1020-49891997000100002
12. W. H. O. Cholera, Weekly epidemiological record, *World Health Organ.*, **82** (2007), 273−284.
13. E. Bertuzzo, L. Mari, L. Righetto, M. Gatto, R. Casagrandi, M. Blokesch, et al., Prediction of the spatial evolution and effects of control measures for the unfolding Haiti cholera outbreak, *Geophys. Res. Lett.*, **38** (2011), L06403. https://doi.org/10.1029/2011GL046823
14. M. Ghosh, J. B. Shukla, P. Chandra, P. Sinha, An epidemiological model for carrier dependent infectious diseases with environmental effect, *Int. J. Appl. Sc. Comp.*, **7** (2000), 188−204.
15. A. Shangbing, Global stability of equilibria in a tick-borne disease model, *Math. Biosci. Eng.*, **4** (2007), 567–572. https://doi.org/10.3934/mbe.2007.4.567
16. N. T. J. Bailey, Spatial models in the epidemiology of infectious diseases, *Lect. Notes Math.*, **38** (1980), 233−261. https://doi.org/10.1007/978-3-642-61850-5_22
17. H. W. Hethcote, Qualitative analysis of communicable disease models, *Math. Biosci.*, **28** (1976), 335−356. https://doi.org/10.1016/0025-5564(76)90132-2
18. P. Das, D. Mukherjee, A. K. Sarkar, Study of carrier dependent infectious disease-cholera, *J. Biol. Syst.*, **13** (2005), 233−244. https://doi.org/10.1142/S0218339005001495
19. S. Singh, P. Chandra, J. B. Shukla, Modeling and analysis of the spread of carrier dependent infectious diseases with environmental effects, *J. Biol. Syst.*, **11** (2003), 325−335. https://doi.org/10.1142/S0218339003000877

20. A. K. Misra, A. Sharma, J. B. Shukla, Modeling and analysis of effects of awareness programs by media on the spread of infectious diseases, *Math. Comput. Model.*, **53** (2011), 1221−1228. https://doi.org/10.1016/j.mcm.2010.12.005
21. V. Capasso, S. L. Paveri-Fontana, A mathematical model for the 1973 cholera epidemic in the European Mediterranean region, *Rev. Epidemiol. Sante*, **27** (1979), 121–132.
22. C. T. Codec-o, Endemic and epidemic dynamics of cholera: The role of the aquatic reservoir, *BMC Infect. Dis.*, **1** (2001), 1. https://doi.org/10.1186/1471-2334-1-1
23. M. Pascual, M. J. Bouma, A. P. Dobson, Cholera and climate: Revisiting the quantitative evidence, *Microbes Infect.*, **4** (2002), 237−245. https://doi.org/10.1016/S1286-4579(01)01533-7
24. M. A. Jensen, S. M. Faruque, J. J. Mekalanos, B. R. Levin, Modeling the role of bacteriophage in the control of cholera outbreaks, *Proc. Natl. Acad. Sci.*, **103** (2006), 4652−4657. https://doi.org/10.1073/pnas.0600166103
25. E. Bertuzzo, S. Azaele, A. Maritan, M. Gatto, I. Rodriguez-Iturbe, A. Rinaldo, On the space-time evolution of a cholera epidemic, *Water Resour. Res.*, **44** (2008), L06403. https://doi.org/10.1029/2007WR006211
26. R. M. Anderson, R. M. May, Vaccination against rubella and measles: Qualitative investigation of different policies, *J. Hyg. Cambridge*, **90** (1983), 259–352. https://doi.org/10.1017/s002217240002893x
27. B. Shulgin, L. Stone, Z. Agur, Pulse vaccination strategy in the SIR epidemic model, *Bull. Math. Biol.*, **60** (1998), 1123–1148. https://doi.org/10.1006/S0092-8240(98)90005-2
28. X. Liu, Y. Takeuchi, S. Iwami, SVIR epidemic models with vaccination strategies, *J. Theor. Biol.*, **253** (2008), 1–11. https://doi.org/10.1016/j.jtbi.2007.10.014
29. R. Naresh, S. Pandey, A. K. Misra, Analysis of a vaccination model for carrier dependent infectious diseases with environmental effects, *Nonlinear Anal. Model. Control*, **13** (2008), 331−350. https://doi.org/10.15388/NA.2008.13.3.14561
30. T. Zhang, Z. Teng, An SIRVS epidemic model with pulse vaccination strategy, *J. Theor. Biol.*, **250** (2008), 375−381. https://doi.org/10.1016/j.jtbi.2007.09.034
31. D. L. Chao, M. E. Halloran, I. M. Longini Jr., Vaccination strategies for epidemic cholera in Haiti with implications for the developing world, *Proc. Natl. Acad. Sci.*, **108** (2011), 7081−7085. https://doi.org/10.1073/pnas.110214910
32. A. R. Tuite, J. Tien, M. Eisenberg, D. J. D. Earn, J. Ma, D. N. Fisman, Cholera epidemic in Haiti, 2010: Using a transmission model to explain spatial spread of disease and identify optimal control interventions, *Ann. Intern. Med.*, **154** (2011), 593−601. https://doi.org/10.7326/0003-4819-154-9-201105030-00334
33. Z. Sabir, Stochastic numerical investigations for nonlinear three-species food chain system, *Int. J. Biomath.*, **15** (2022), 2250005. https://doi.org/10.1142/S179352452250005X
34. Z. Sabir, T. Botmart, M.A.Z. Raja, R. Sadat, M.R. Ali, A.A. Alsulami, et al., Artificial neural network scheme to solve the nonlinear influenza disease model, *Biomed. Signal Proces.*, **75** (2022), 103594. https://doi.org/10.1016/j.bspc.2022.103594
35. M. Umar, Z. Sabir, M. A. Z. Raja, M. Shoaib, M. Gupta, Y. G. Sánchez, A stochastic intelligent computing with neuro-evolution heuristics for nonlinear SITR system of novel COVID-19 dynamics, *Symmetry*, **12** (2020), 1628. https://doi.org/10.3390/sym12101628

36. M. Umar, Z. Sabir, F. Amin, J. L. Guirao, M. A. Z. Raja, Stochastic numerical technique for solving HIV infection model of $CD4^+$ T cells, *Eur. Phys. J. Plus*, **135** (2020), 403. https://doi.org/10.1140/epjp/s13360-020-00417-5
37. Z. Sabir, Neuron analysis through the swarming procedures for the singular two-point boundary value problems arising in the theory of thermal explosion, *Eur. Phys. J. Plus*, **137** (2022), 638. https://doi.org/10.1140/epjp/s13360-022-02869-3
38. B. Wang, J. F. Gomez-Aguilar, Z. Sabir, M. A. Z. Raja, W. F. Xia, H. Jahanshahi, et al., Numerical computing to solve the nonlinear corneal system of eye surgery using the capability of Morlet wavelet artificial neural networks, *Fractals*, **30** (2022), 2240147. https://doi.org/10.1142/S0218348X22401478
39. M. Umar, F. Amin, H. A. Wahab, D. Baleanu, Unsupervised constrained neural network modeling of boundary value corneal model for eye surgery, *Appl. Soft Comput.*, **85** (2019), 105826. https://doi.org/10.1016/j.asoc.2019.105826
40. Z. Sabir, H. A. Wahab, Evolutionary heuristic with Gudermannian neural networks for the nonlinear singular models of third kind, *Phys. Scr.*, **96** (2021), 125261. https://doi.org/10.1088/1402-4896/ac3c56
41. T. Saeed, Z. Sabir, M. S. Alhodaly, H. H. Alsulami, Y. G. Sánchez, An advanced heuristic approach for a nonlinear mathematical based medical smoking model, *Results Phys.*, **32** (2022), 105137. https://doi.org/10.1016/j.rinp.2021.105137
42. A. K. Misra, V. Singh, A delay mathematical model for the spread and control of water borne diseases, *J. Theor. Biol.*, **301** (2012), 49−56. https://doi.org/10.1016/j.jtbi.2012.02.006
43. Z. Sabir, M. A. Z. Raja, M. Shoaib, J. F. Aguilar, FMNEICS: Fractional Meyer neuro-evolution-based intelligent computing solver for doubly singular multi-fractional order Lane-Emden system, *Comp. Appl. Math.*, **39** (2020), 303. https://doi.org/10.1007/s40314-020-01350-0
44. H. Günerhan, E. Çelik, Analytical and approximate solutions of fractional partial differential-algebraic equations, *Appl. Math. Nonlinear Sci.*, **5** (2020), 109−120. https://doi.org/10.2478/amns.2020.1.00011
45. K. A. Touchent, Z. Hammouch, T. Mekkaoui, A modified invariant subspace method for solving partial differential equations with non-singular kernel fractional derivatives, *Appl. Math. Nonlinear Sci.*, 5 (2020), 35−48. https://doi.org/10.2478/amns.2020.2.00012
46. Z. Sabir, M. A. Z. Raja, J. L. Guirao, T. Saeed, Meyer wavelet neural networks to solve a novel design of fractional order pantograph Lane-Emden differential model, *Chaos Soliton. Fract.*, **152** (2021), 111404. https://doi.org/10.1016/j.chaos.2021.111404
47. E. İlhan, İ. O. Kıymaz, A generalization of truncated M-fractional derivative and applications to fractional differential equations, *Appl. Math. Nonlinear Sci.*, **5** (2020), 171−188. https://doi.org/10.2478/amns.2020.1.00016
48. H. M. Baskonus, H. Bulut, T. A. Sulaiman, New complex hyperbolic structures to the lonngren-wave equation by using sine-gordon expansion method, *Appl. Math. Nonlinear Sci.*, **4** (2019), 129−138. https://doi.org/10.2478/AMNS.2019.1.00013
49. T. Botmart, N. Yotha, P. Niamsup, W. Weera, Hybrid adaptive pinning control for function projective synchronization of delayed neural networks with mixed uncertain couplings, *Complexity*, **2017** (2017), 4654020. http://dx.doi.org/10.1155/2017/4654020

50. T. Botmart, W. Weera, Guaranteed cost control for exponential synchronization of cellular neural networks with mixed time-varying delays via hybrid feedback control, *Abstr. Appl. Anal.*, **2013** (2013), 175796. https://doi.org/10.1155/2013/175796
51. P. Lakshminarayana, K. Vajravelu, G. Sucharitha, S. Sreenadh, Peristaltic slip flow of a Bingham fluid in an inclined porous conduit with Joule heating, *Appl. Math. Nonlinear Sci.*, **3** (2018), 41−54. https://doi.org/10.21042/AMNS.2018.1.00005
52. T. Sajid, S. Tanveer, Z. Sabir, J. L. G. Guirao, Impact of activation energy and temperature-dependent heat source/sink on maxwell-sutterby fluid, *Math. Probl. Eng.*, **2020** (2020), 5251804. https://doi.org/10.1155/2020/5251804
53. R. Ahmad, A. Farooqi, J. Zhang, N. Ali, Steady flow of a power law fluid through a tapered non-symmetric stenotic tube, *Appl. Math. Nonlinear Sci.*, **4** (2019), 255−266. https://doi.org/10.2478/AMNS.2019.1.00022
54. N. Moslemi, B. Abdi, S. Gohari, I. Sudin, E. Atashpaz-Gargari, N. Redzuan, et al., Thermal response analysis and parameter prediction of additively manufactured polymers, *Appl. Therm. Eng.*, **212** (2022), 118533. https://doi.org/10.1016/j.applthermaleng.2022.118533
55. N. Moslemi, S. Gohari, B. Abdi, I. Sudin, H. Ghandvar, N. Redzuan, et al., A novel systematic numerical approach on determination of heat source parameters in welding process, *J. Mater. Res. Technol.*, **18** (2022), 4427−4444. https://doi.org/10.1016/j.jmrt.2022.04.039
56. N. Moslemi, B. Abdi, S. Gohari, I. Sudin, N. Redzuan, A. Ayob, et al., Influence of welding sequences on induced residual stress and distortion in pipes, *Constr. Build. Mater.*, **342** (2022), 127995. https://doi.org/10.1016/j.conbuildmat.2022.127995

AIMS Press